Does Nitric Acid Dissociate at the Aqueous Solution Surface?

ARTICLE *in* THE JOURNAL OF PHYSICAL CHEMISTRY C · SEPTEMBER 2011

Impact Factor: 4.77 · DOI: 10.1021/jp205842w

THE JOURNAL OF PHYSICAL CHEMISTRY C

ARTICLE

pubs.acs.org/JPCC

Does Nitric Acid Dissociate at the Aqueous Solution Surface?

Tanza Lewis,[†] Bernd Winter,[‡] Abraham C. Stern,[†] Marcel D. Baer,[§] Christopher J. Mundy,[§] Douglas J. Tobias,[†] and John C. Hemminger*[,†]

[†]Department of Chemistry, University of California, Irvine, California 92697, United States

[‡]Helmholtz-Zentrum Berlin für Materialien und Energie, and BESSY, D-12489 Berlin, Germany

[§]Chemical and Materials Sciences Division, Pacific Northwest National Laboratory, Richland, Washington 99352, United States

ABSTRACT: Nitric acid is a prevalent component of atmospheric aerosols, and the extent of nitric acid dissociation at aqueous interfaces is relevant to its role in heterogeneous atmospheric chemistry. Several experimental and theoretical studies have suggested that the extent of dissociation of nitric acid near aqueous interfaces is less than that in bulk solution. Here dissociation of HNO_3 at the surface of aqueous solution is quantified using X-ray photoelectron spectroscopy of the nitrogen local electronic structure. The relative amounts of undissociated $HNO_3(aq)$ and dissociated $NO_3^-(aq)$ are identified by the distinguishable N1s core-level photoelectron spectra of the two species, and we determine the degree of dissociation, α_{int}, in the interface (approximately the first three layers of solution) as a function of HNO_3 concentration. Our measurements show that dissociation is decreased by ~20% near the solution interface compared with bulk solution and furthermore that dissociation occurs in the topmost solution layer. The experimental results are supported by first-principles MD simulations, which show that hydrogen bonds between HNO_3 and water molecules at the solution surface stabilize the molecular form even at low concentration by analogy to the stabilization of molecular HNO_3 that occurs in bulk solution at high concentration.

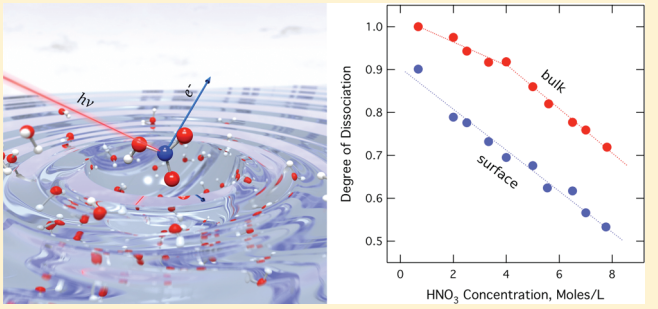

INTRODUCTION

Dissociation of nitric acid at the liquid/vapor interface of aqueous solution is of particular interest to the atmospheric chemistry community[1−10] and is a process that is yet to be fully understood on the molecular level. Regarding the role of nitric acid in atmospheric aerosol, it has been shown that molecular nitric acid on aqueous surfaces undergoes renoxification to form NO_2 gas and subsequent photochemically active nitrogen species.[3,4,6,7] Nitric acid is also important in the aging processes that occur in sea salt particles.[2,5] Recent sum frequency generation (SFG) studies[1,8] have clearly shown that undissociated nitric acid exists at the surface of nitric acid aqueous solution. Reference 8 suggests the existence of two different hydrogen-bonded species of HNO_3, one residing at the solution surface and a second deeper in the interface, differing in the degree of solvation of the nitro group. Theoretical studies have shed light on the mechanism of HNO_3 dissociation at an aqueous interface versus in bulk solution.[9−11] For example, ref 10 characterizes the solvation dynamics that are important for HNO_3 acid dissociation (specific parameters include the distance between HNO_3 and proton-accepting H_2O, coordination of the proton-accepting H_2O, and solvation of resulting NO_3^-) and proposes that proton transfer (PT) in the interfacial region occurs when these parameters are changed from their optimal values in the bulk because of microsolvation effects in the interfacial region.

In this work, we apply X-ray photoelectron (PE) spectroscopy to the dissociation of nitric acid in water, that is, the proton-transfer reaction

$$HNO_3(aq) + H_2O(aq) \rightarrow H_3O^+(aq) + NO_3^-(aq) \quad (1)$$

and our focus is on the process at the solution interface. It has been previously shown that undissociated nitric acid exists at the surface (top layer) of solution,[1,8] and the main question to be addressed here is to what extent HNO_3 dissociates in the vicinity of the water surface. We report the first direct measurement of the degree of dissociation of HNO_3 in the interfacial region. Our X-ray PE measurements are complementary to SFG studies in the sense that both techniques are capable of detecting undissociated nitric acid at the solution surface. However, our measurements enable us to go a step further and quantify the relative amounts of molecular and dissociated forms of HNO_3 present in the interfacial region. Experimentally, surface-sensitive PE spectroscopy measurements require that the inelastic mean free path (IMFP) of the PEs detected is minimal, which is the case when electron kinetic energies (eKE) are near 60−100 eV.[12] N1s spectra from nitric acid solutions in the present surface study were acquired with 500 eV photon energy, resulting in 90 eV

Received: June 22, 2011
Revised: September 2, 2011
Published: September 07, 2011

eKE. The estimated minimum probing depth into the solution is ~20 Å (although efforts to determine accurate values of IMFP in water are ongoing),[13] and here we measure the nitrogen 1s PE spectra from nitric-acid solution interfaces. HNO_3(aq) and NO_3^-(aq) can be distinguished by their different electron binding energies (BEs), and with careful consideration of experimental parameters, we determine the relative surface concentration of the two species from the measured N1s signal intensities.

In contrast with the predictions of theoretical studies, our PE spectroscopy experiments suggest that dissociation does in fact occur at the surface (very top layer of solution) as well as throughout the solution interface (approximately the first three layers of solution). In support of these results, we present first-principles MD simulations of HNO_3 at and near the air−water interface as well as in the bulk. The simulations reveal favorable HNO_3−water interactions at and near the interface that are observed in bulk solution only at high concentration, where dissociation is known to be suppressed.

METHODS

Experimental Section. Photoemission measurements were performed from a 15 μm sized liquid vacuum jet at the soft-X-ray U41 PGM undulator beamline of BESSY, Berlin.[14] The jet velocity was ~50 ms^{-1}, and jet temperature was 4 °C. Electrons were detected normal to both the synchrotron-light polarization vector and the flow of the liquid jet. A 100 μm diameter orifice that forms the entrance to the hemispherical electron energy-analyzer is at approximately 0.5 mm distance from the liquid jet. This is short enough to ensure that detected electrons have not suffered from inelastic scattering with water gas-phase molecules around the small sized liquid jet. Under operation conditions the pressure in the interaction chamber was ~1.5×10^{-4} mbar. This implies efficient evaporative cooling. However, the effect is counteracted by the continuous rapid replacement of liquid, which warrants local thermodynamic equilibrium because molecular level mixing occurs on a much slower time scale. As a result, the degree of dissociation determined in the current study will be essentially the same as one would measure for the water/air system. Notice that our previously determined values for the dissociation of nitric acid as a function of concentration in bulk aqueous solution[15] are indeed in accurate agreement with the results of conventional bulk spectroscopic measurements performed under ambient conditions. The energy resolution of the U41 beamline is better than 200 meV at the incident photon energy 500 eV used here, and the resolution of the hemispherical energy analyzer is constant with kinetic energy (~200 meV at 20 eV pass energy). The small focal size, 23 × 12 μm^2, of the incident photon beam allows for matching spatial overlap with the liquid microjet, reducing the gas-phase contributions of the measured spectra to <5%. The aqueous solutions were prepared from 70% HNO_3 in water (<5 ppm inorganic residue; Sigma Aldrich), diluted in highly demineralized water (conductivity ~0.2 mS/cm). HNO_3 concentrations of 0.7−7.8 M were studied here.

COMPUTATIONS

Simulations were carried out using the CP2K software suite (http://cp2k.berlios.de). The forces were computed via the QuickStep module, which contains an accurate and efficient implementation of density functional theory using dual basis sets of Gaussian type orbitals (TZV2P) and plane waves (expanded to

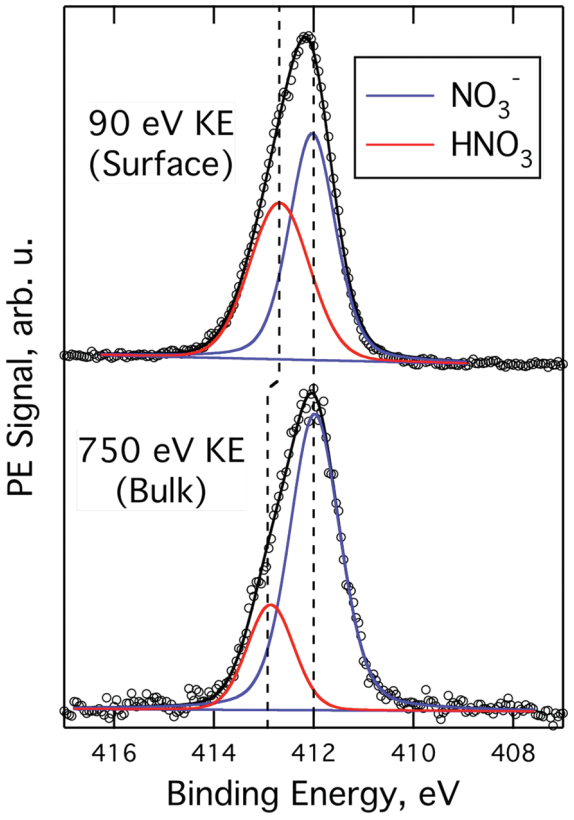

Figure 1. N1s photoelectron spectra of 7.8 M nitric acid aqueous solution measured at 500 and 1157 eV photon energy, resulting in kinetic energies of emitted electrons as indicated, and representing surface and bulk probes, respectively. The two Gaussians highlight relative signal contribution of molecular HNO_3 and dissociated NO_3^- to the total N1s intensity.

E_{cut} = 280 Ry) for the electron density.[16] Only the valence electrons were considered explicitly, and the core−electron states were represented via Goedecker−Teter−Hutter pseudopotentials.[17] The Grimme dispersion correction was used in conjunction with the Becke exchange and Lee−Yang−Parr correlation (BLYP) functional.[18−20] It has been demonstrated that the BLYP/TZV2P theoretical model provides a reasonable description of the effects of solvation for systems that involve PT compared with the higher level MP2/TZV2P model.[21] The dispersion correction to BLYP (BLYP-D) has recently been shown to improve vastly the thermodynamic properties of water under near-ambient conditions over the original uncorrected BLYP description.[22−25]

All of the systems simulated using FPMD consisted of 1 HNO_3 molecule and 216 water molecules in a 15 Å × 15 Å × 71.44 Å box with periodic boundary conditions applied in three dimensions, resulting in a slab of aqueous solution ~31 Å thick with a nominal bulk concentration [HNO_3] ~0.25 M. The system size is large enough to support stable air−water interfaces.[26,27] Three solutions of nitric acid were prepared in which the HNO_3 was positioned at the surface, in the interface approximately two molecular layers of water below the surface, and in the bulk (~15 Å below the surface). We also compare our present results with what we refer to as "true bulk" simulations, which are our previous simulations of aqueous solutions of nitric acid performed with 3D periodic boundary conditions, that is, without solution−vacuum interfaces.[15] All of the simulations were performed in the canonical ensemble at 300 K by coupling

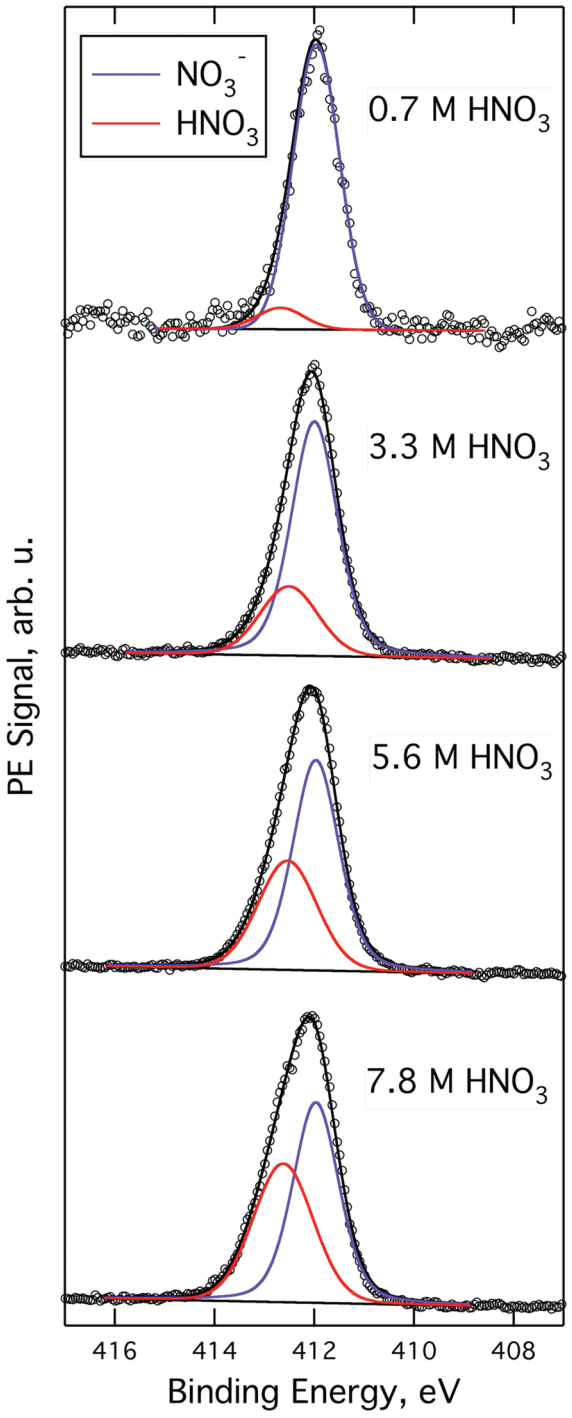

Figure 2. N1s photoelectron spectra of nitric acid aqueous solution interface measured at different bulk concentrations. The two Gaussians highlight signal from molecular HNO_3 and from NO_3^-, respectively.

Nosé−Hoover chain thermostats with characteristic frequencies of 2000 cm^{-1} to every degree of freedom.[28] The time step of the simulations was 0.5 fs. At each time step, the wave function was minimized to a tolerance of 10^{-6} H.

RESULTS AND DISCUSSION

Figure 1 shows N1s PE spectra from 7.8 M nitric acid aqueous solution measured at 500 and 1157 eV photon energy (90 and

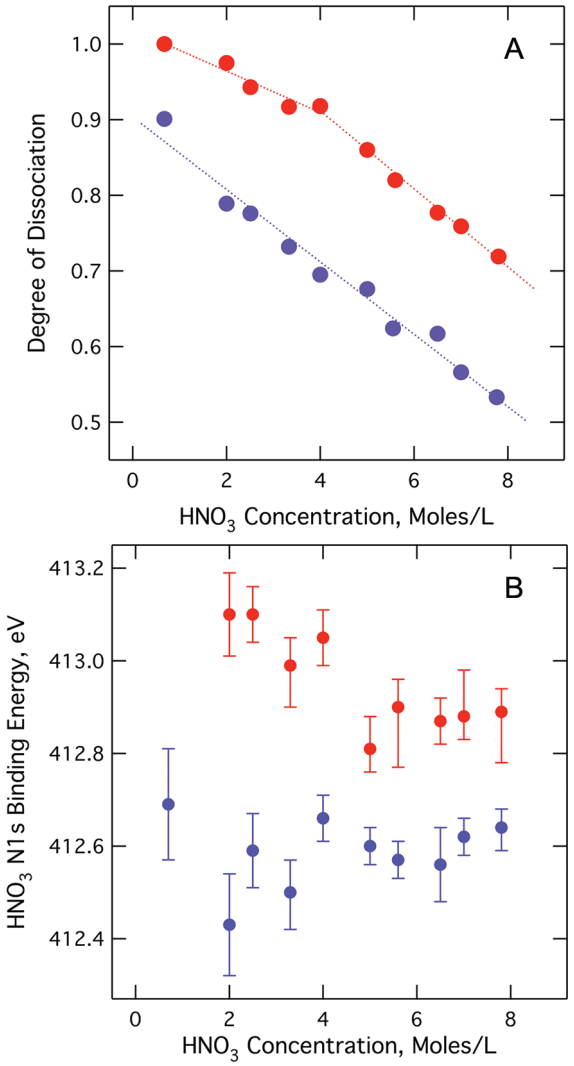

Figure 3. (a) Degree of nitric acid dissociation in bulk solutions (α, in red) and at the solution interface (α_{int}, in blue) as a function of concentration. (b) N1s binding energy of HNO_3(aq) in bulk solution (red) and at the solution surface (blue) as a function of nitric acid bulk concentration.

750 eV eKE, respectively). N1s BEs are presented with respect to vacuum and were calibrated by the valence-band $1b_1$ BE of water.[29] We can distinguish two contributions to the N1s PE spectrum, represented here by Gaussians, yielding a good total fit to the experimental spectrum. Spectral fitting parameters will be described below. The higher-energy component (in red), at ~413 eV BE, is due to the photoemission from undissociated HNO_3(aq), and the component at 412 eV BE (in blue) is from NO_3^-(aq). The higher BE for HNO_3(aq) essentially results from charge withdrawal away from the nitrogen site, leading to lower electron density. The observed larger ratio of HNO_3/NO_3^- PE signals for 500 eV than for 1157 eV photons is a consequence of probing the surface at the lower photon energy (resulting in minimal IMFP), whereas the higher photon energy probes primarily electrons from bulk solution. The BE of HNO_3(aq) is slightly higher in bulk solution than in the interfacial region, and this is related to the experimental probe depth that we will discuss later in detail. The important note here is that Figure 1 immediately shows that we detect molecular

HNO_3 present in the interface and that dissociation is reduced in the interface when compared with bulk solution. From Figure 1 alone, however, we cannot yet infer the extent of dissociation for top-layer surface configurations.

Figure 2 shows N1s PE spectra from the interface of nitric acid aqueous solution for 0.7, 3.3, 5.6, and 7.8 M; the latter is identical to the spectrum shown in Figure 1(top). The two Gaussians (in red and blue) again represent signal from molecular HNO_3 and from NO_3^-, respectively. In 0.7 M nitric acid solution, we detect a small signal from undissociated acid present at the interface, and the HNO_3(aq) signal continues growing with increasing nitric acid concentration. To deconvolute each spectrum, we keep the full width half-maximum (fwhm) of the NO_3^- peak fixed to the width of NO_3^- in dilute nitric acid (see 0.7 M nitric acid) or aqueous nitrate solutions (fwhm = 1.2 eV). We allow peak position and magnitude to vary and fit additional intensity due to molecular HNO_3 with a second Gaussian (in red) of fwhm = 1.4 eV. The nitrogen 1s PE intensity ratios in Figure 2 are a fairly accurate measure of the relative concentrations of HNO_3 and NO_3^- in the solution interface (which will later be justified), and for each concentration, we can determine the experimental value of α_{int}, the extent of dissociation in the interfacial region, within limits of signal-to-noise.

Values of α_{int} obtained from the integrated PE spectra presented in Figure 2 are plotted in Figure 3a (blue circles) along with α (= α_{bulk}), the bulk degree of dissociation reported in previous work.[15] Experimental error corresponds to the size of the circles shown and primarily originates from small uncertainties in solution concentration as well as from low HNO_3 signal-to-noise ratio at lower concentrations. We find that values of α_{int} are, on average, ~20% smaller than α over the concentration range studied. Therefore, Figure 3a clearly shows that nitric acid is less dissociated at the solution interface than in bulk solution throughout the entire concentration range considered. Curiously, α_{int} appears to vary linearly with bulk nitric acid concentration, although we are unable to explain the origin of linearity based on the present experiments. Next, we carefully scrutinize our experimental parameters to determine the extent of dissociation at the topmost layer of the solution surface.

We now discuss the reliability of our measured values of α_{int}, how deeply into the solution interface our experiment probes, and how this relates to whether HNO_3 in the top layer of solution dissociates by considering the origin of the measured PE signal in further detail. PE spectroscopy detects PEs emerging from a distance z into the solution, where the measured PE signal is an integration of contributions into the solution, weighted by the exponentially decaying attenuation length, which depends on IMFP.[13] Hence any PE measurement will detect weighted signal from the surface, with a weight that decreases with increasing IMFP. Unfortunately, for aqueous solutions, the IMFP is not well-known, and we have to rely on reasonable assumptions for our interfacial measurements, as we shall show below. We also need to mention that we currently have a poor understanding of the angle dependence of the emitted PEs at solution interfaces, and anisotropy parameters[13] are unknown for these systems. However, in the present study, where we compare the electron emission from the same orbital symmetry (1s), we believe that differences in anisotropies are too small to affect the qualitative conclusions.

One crucial piece of experimental information relevant to determining whether HNO_3 dissociates at the solution surface comes from the electronic structure changes of the nitrogen local

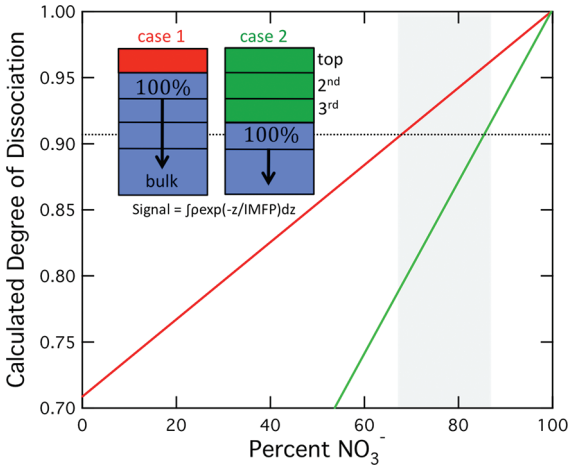

Figure 4. Predicted α_{int} values obtained from varying the percent NO_3^- in the first layer(s) of solution for two simple test cases. Expected signals are calculated using the equation shown (ρ = density of species, z = layers into solution, IMFP = inelastic mean free path).

environment (N1s chemical shifts) associated with the location of HNO_3 with respect to the solution surface. Comparison of the N1s BEs obtained for surface-sensitive (Figure 2) and bulk (previously published)[15] measurements as a function of bulk nitric acid concentration is shown in Figure 3b. The HNO_3 N1s BE is consistently lower for the interfacial measurements than for any bulk solution measurement. (The BE difference is marked in Figure 1 for 7.8 M concentration.) Hence, we can experimentally distinguish HNO_3 molecules at these distinctively different locations by their N1s BE, where the higher-BE species detected in bulk solution are completely absent in the surface-sensitive measurements. We argue, therefore, that our experimental probe depth must be comparable to the length of the solution interface, where HNO_3 will exhibit different solvation configurations than in bulk solution. Interestingly, the interfacial HNO_3 BE remains constant with concentration, suggesting perhaps that the HNO_3 interfacial solvent structure remains somewhat similar regardless of changes in bulk concentration.

Because the probing depth in the present experiment is essentially the length of the solution interface (the absolute length in units of angstroms is unknown), we cannot easily distinguish between contributions from top layer and subsurface layers, and we therefore have to test several assumptions. Specifically, we will test out an interfacial composition model in its ability to reproduce quantitatively the dissociation curve of Figure 3a, and here we need to express the dimension of the interface by some meaningful measure. In our simple model, we assume an IMFP of three interfacial layers (top, second, third), a choice motivated by the occurrence of characteristic HNO_3 interfacial hydration configurations found in previous MD simulations.[10] Configurations at larger depth, that is, deeper than the third layer, are considered to be bulk structures. We note, however, that the qualitative conclusions from our model will still hold true if we choose an IMFP larger than three layers. Our analysis focuses on the special case of low nitric acid concentration, and here we refer to our measurement of 0.7 M nitric acid (shown in Figure 3a), where we observe 100% dissociation in bulk solution yet detect undissociated acid present in the solution interface and measure α_{int} = 0.91 (i.e., 9% undissociated HNO_3). In Figure 4, we apply two simple tests

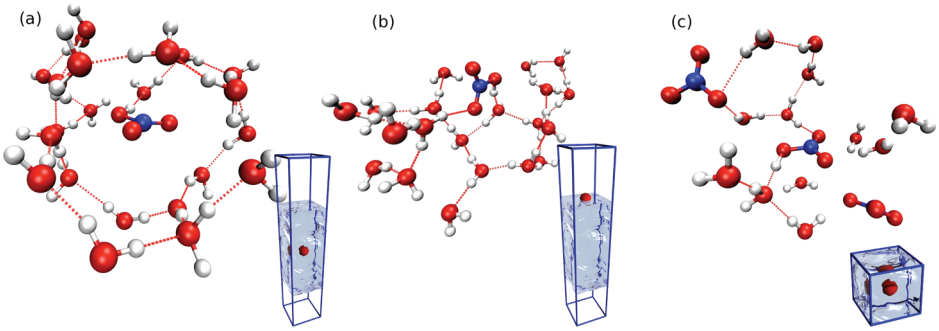

Figure 5. Representative snapshots of infinitely dilute undissociated HNO_3 in (a) the bulk of a water slab, (b) the surface of a water slab, and (c) a representative snapshot of HNO_3 at 5 M concentration in bulk simulation.

to our model and plot the predicted α_{int} as we vary the percentage of NO_3^- present in the top layer(s) of solution. First (schematic and line shown in red, case 1), we examine the case where nitric acid dissociates completely beginning in the second layer, assuming that any change in dissociation occurs exclusively in the topmost layer. This should allow us to assess the prediction made by previous theoretical simulations that even in the infinitely dilute case zero dissociation occurs here. However, with zero percent NO_3^-, that is, zero dissociation at the top layer, our model predicts that α_{int} should be ~0.7, which is significantly lower than our experimentally measured value of 0.91. We predict only an α_{int} that is consistent with our experiment when the topmost layer contains 65% NO_3^-(aq). We conclude immediately from this analysis that dissociation must occur to some extent at the top layer of solution. Next, we examine a second case (schematic and line shown in green, case 2) where we assume that equal dissociation occurs throughout the first three layers of solution, that is, the interface, with complete dissociation beginning in layer 4. This should provide an upper bound for quantifying dissociation in the solution interface. Here α_{int} approaches our experimentally determined value when the first three layers are composed of 85% NO_3^-(aq). From our experiments, we cannot say whether the undissociated HNO_3 exists exclusively in the top layer or throughout the first three layers of solution, but we can conclude that in any case significant dissociation must occur at the solution surface. From the two "extreme" cases tested here, we suggest that the top layer of solution is composed of 65−85% NO_3^-(aq) at low concentrations, acknowledging that the actual situation may be intermediate. Even if we allow for more generous assumptions on IMFP (and hence probing depth), the conclusion of top-layer dissociation, although to lesser extent, would hold with our current model until IMFP approaches 15 solvent layers. However, an IMFP of 15 layers would mean probing into bulk solution and is certainly well beyond our minimum experimental probe depth in the current measurements. We therefore consider our simple test model to be robust, even considering uncertainties in exact probing depth.

Our modeling of the depth-dependence of the PE signal leads to the conclusion that although dissociation is reduced at the interface, it does occur to some extent at the very top layer of the solution. We note that although our experiment does not reveal the explicit solvent structure changes encountered at the surface, at the interface, and in the bulk solution our data suggest that HNO_3 solvation in the interface is different from bulk HNO_3 solvation. Additional insight into interfacial versus bulk solvation can be gleaned from our first-principles MD simulations. Figure 5a depicts a representative snapshot from an MD simulation of an undissociated HNO_3 molecule (infinite dilution) in the bulk of a water slab (216 waters; see details in Methods section). The hydration structure can be described as a clathrate-like structure around HNO_3, in which there is only a single HNO_3−water hydrogen bond, with HNO_3 donating a proton to a water oxygen acceptor. In previous work,[15] we have shown that at low HNO_3 concentration water−water hydrogen bonds are formed at the expense of HNO_3−water hydrogen bonds in the solvation shell of HNO_3. Such a solvation structure is apparently less energetically favorable than that of the two ionic products, which have similar solvation structures over a wide range of HNO_3 concentration. We hypothesized, therefore, that HNO_3 is destabilized relative to its ionic dissociation products at low concentration because of reduced favorable interactions with water molecules in its solvation shell. Moreover, we have described molecular HNO_3 at low concentration as being hydrophobic.

Figure 5b depicts a representative snapshot from an MD simulation in which a single HNO_3(aq) molecule is located in the topmost layer of the same water slab. It is obvious from the snapshot that the clathrate-like structure observed in the bulk is not evident at the surface of the slab. Rather, it appears that water and HNO_3 interact more strongly at the solution surface, as evidenced by an additional hydrogen bond formed to an unprotonated oxygen of HNO_3. The hydrogen-bonded structure identified here may resemble configurations proposed by SFG experiments and observed in previous theoretical calculations.[8,10] Curiously, the change in solvation structure observed between bulk (Figure 5a) and surface (Figure 5b) HNO_3 is similar to the change we observed previously when comparing solvation configurations at low and high concentration HNO_3(aq) in bulk solution: at high concentrations (>4 M), crowding of solvent shells due to additional NO_3 moieties leads to the breakdown of the clathrate-like water network around HNO_3 and results in the formation of an additional hydrogen bond between an unprotonated oxygen of HNO_3 and water. (See the snapshot in Figure 5c.) However, before we draw further conclusions from the comparison of HNO_3 in surface and high-concentration bulk environments and relate this to whether HNO_3 dissociates at the solution surface, we need to consider the structure and orientation of surface HNO_3 in greater detail.

In the present simulations, we characterize the observed orientations of HNO_3 at the aqueous surface throughout the simulation trajectory by calculating the angle between the surface normal and a vector drawn from the HNO_3 protonated oxygen to

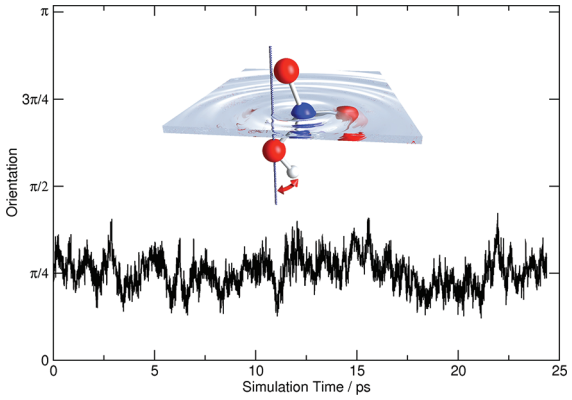

Figure 6. HNO_3 proton orientation, calculated as the angle between the surface normal vector and a vector that points from HNO_3 protonated oxygen to the proton, shown as a function of simulation trajectory time.

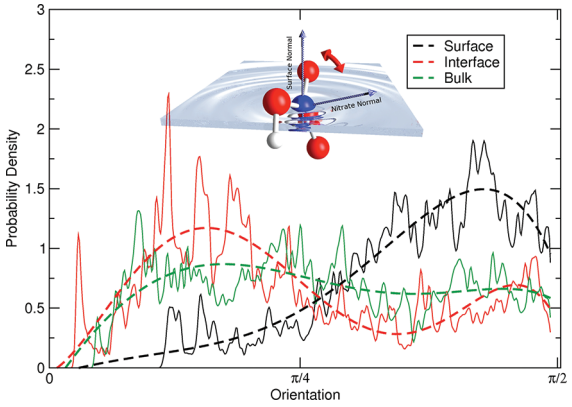

Figure 7. Probability distribution of NO_3 orientations, calculated as the angle between the surface normal vector and a vector that is normal to the plane of the nitrate.

the proton. This allows us to characterize the direction that the proton points, where 0° corresponds to the proton pointing directly into the bulk solution. The time evolution of the angle during the simulation of HNO_3 in the topmost layer of the slab is shown in Figure 6. We see that the orientation of the HNO_3 proton remains surprisingly constant at ∼30° with respect to the surface normal during the entire simulation. This corresponds to the proton pointing directly to the solution and suggests a preference for proton solvation by donating a hydrogen bond to well-solvated water molecules. To characterize further the orientation of HNO_3 at the surface of the slab, we also consider the orientation of the NO_3 moiety, expressed here as the orientation of the vector normal to the NO_3 plane with respect to the surface normal, shown in Figure 7. At the solution surface, HNO_3 molecules have a very high probability of being oriented almost 90° from the surface normal. This suggests that the orientation of surface $HNO_3(aq)$ previously shown in the snapshot (Figure 5b) is indeed representative of HNO_3 structure throughout the simulation. Also shown in Figure 7 is the orientation of HNO_3 residing in bulk solution (for which we see an almost uniform distribution, as expected) and in the vicinity the solution interface (∼7 Å below the solution surface). Near the interface, HNO_3 exhibits a slight preference for being oriented ∼30° from the surface normal.

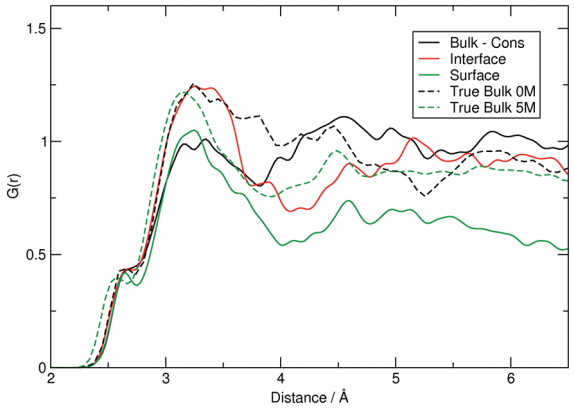

Figure 8. Radial distribution functions computed from nitrate oxygen of HNO_3 to water oxygen shown for several systems.

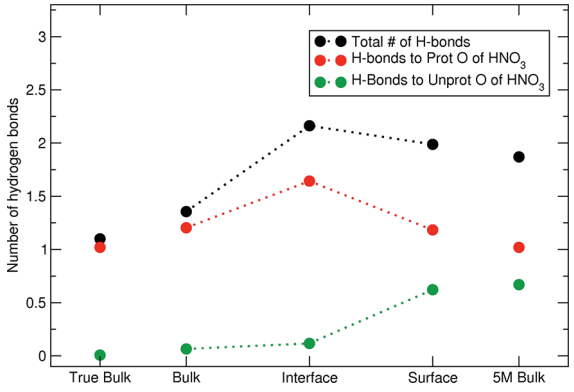

Figure 9. Number of hydrogen bonds formed between water and HNO_3 in various environments.

Now that we have analyzed the preferential orientation of undissociated HNO_3 at the solution surface, we return to a discussion of HNO_3 solvation and hydrogen bonding. To characterize HNO_3 solvation structures, we calculate the radial distribution function (RDF) of water around the oxygen atoms of nitric acid. The results are shown in Figure 8 for HNO_3 in various settings. For dilute HNO_3 in bulk solution, the RDF is relatively unstructured. This is consistent with the clathrate-like solvation structure depicted in the MD snapshot (Figure 5a). In contrast, the RDFs for undissociated $HNO_3(aq)$ in the interface and at the solution surface are relatively well-structured (with a clear minimum around 4 Å), which is indicative of a more defined solvation shell. Note that a very similarly structured RDF was previously observed for $HNO_3(aq)$ at high concentration in bulk solution.[15] The RDFs presented here are a measure of the enhancement of the local density of water around HNO_3 relative to the bulk density, but they do not provide direct information on specific interactions, for example, hydrogen bonds. To provide additional insight into HNO_3−water interactions, we report the average number of hydrogen bonds between HNO_3 and water in each system in Figure 9. Hydrogen bonding to HNO_3 is relatively scarce. In dilute bulk solution, $HNO_3(aq)$ donates one hydrogen bond, the HNO_3 proton to water oxygen, and accepts none. However, dilute HNO_3 in the interface and at the solution surface participates in an additional hydrogen bond, preferentially formed to an unprotonated oxygen (c.f. the snapshots in Figure 5). We conclude that at the solution surface, because of

limitations of hydrogen-bonding opportunities, water molecules are enticed to interact more strongly with the moderately hydrophobic HNO_3 species. The increase in HNO_3−water hydrogen bonding at the solution interface is analogous to that observed at high bulk HNO_3 concentration, where water−water hydrogen bonding is similarly suppressed because of the relative paucity of opportunities.

We have seen that HNO_3 at the solution surface and in concentrated bulk solution displays a similar tendency toward more structured solvation and an increased degree of hydrogen bonding compared with HNO_3 in dilute bulk solution. In both cases (surface and high concentration bulk), water is relatively scarce. At high concentrations, this is the result of crowding from additional NO_3 moieties in solution and, likewise, at the solution surface the scarcity of water is a direct consequence of reduced density at the liquid/vapor interface. We suggest that an insufficient amount of water around HNO_3 is the driving force for the observed stronger hydrogen bond interaction. Importantly, the lack of sufficient water molecules in each case results in almost identical hydrogen bonding configurations, and here we make a qualitative argument for dissociation at the solution surface. It is well known from previous studies, and confirmed by the experiments reported herein, that the dissociation of nitric acid decreases with increasing concentration. We argue that the solvation of HNO_3 at the solution interface, which is similar to that observed in concentrated bulk HNO_3, stabilizes the molecular form relative to its ionic dissociation products to a greater extent than in dilute bulk nitric acid.

CONCLUSIONS

Dissociation of nitric acid at the surface of aqueous solutions was investigated on the molecular level. We presented the first direct experimental measurements of the degree of dissociation of HNO_3 at the water surface, which show that HNO_3 is on average ∼20% less dissociated in the solution interface when compared with bulk solution. Furthermore, we showed that dissociation must be nonzero at the top layer of solution surface. We characterized surface solvation configurations of undissociated HNO_3 through first-principles MD simulations, which revealed a more structured solvent shell and increased hydrogen bonding to HNO_3 at the surface of a water slab versus in dilute nitric acid bulk solution. Interestingly, these tendencies are closely analogous to changes in hydrogen bonding configurations that were observed in high-concentrations of bulk nitric acid, where fairly strong dissociation is known to occur. By analogy to the qualitatively very similar solvation structures in the high concentration case, we argue that solvation configurations at the solution surface support dissociation, although to a lesser extent than in dilute bulk solution.

AUTHOR INFORMATION

Corresponding Author

*E-mail: jchemmin@uci.edu. Tel: 949-824-5796. Fax: 949-824-2095.

ACKNOWLEDGMENT

AirUCI under Grant CHE 0431312 from the NSF supported this work. Additional support from the Deutsche Forschungsgemeinschaft (Project WI 1327/3-1) is gratefully acknowledged. The work at Pacific Northwest National Laboratory (PNNL) was performed under the auspices of the Division of Chemical Sciences, Geosciences, and Biosciences, Office of Basic Energy Sciences, U.S. Department of Energy, under contract number DE-AC06-76RLO 1830 with Battelle Memorial Institute, which operates PNNL. The molecular dynamics simulations utilized the BlueGene/P at Argonne National Laboratory (resources of the Argonne Leadership Computing Facility at Argonne National Laboratory, which is supported by the Office of Science of the U.S. DOE under Contract No. DE-AC02-06CH11357) under an INCITE 2007-2010 award as well a computational resources from the National Energy Research Supercomputing Center (NERSC) at Lawrence Berkeley National Laboratory, the Molecular Sciences Computing Facility at PNNL, and the University of California Shared Research Computing Services (ShaRCS) pilot project. M.D.B. is grateful for the support of the Linus Pauling Distinguished Postdoctoral Fellowship program at PNNL. We also thank Manfred Faubel and Matthew A. Brown for their contributions to various aspects of this work.

REFERENCES

(1) Schnitzer, C.; Baldelli, S.; Campbell, D. J.; Shultz, M. J. *J. Phys. Chem. A* **1999**, *103*, 6383.
(2) Finlayson-Pitts, B. J.; Hemminger, J. C. *J. Phys. Chem. A* **2000**, *104*, 11463.
(3) Mochida, M.; Finlayson-Pitts, B. J. *J. Phys. Chem. A* **2000**, *104*, 9705.
(4) Saliba, N. A.; Yang, H.; Finlayson-Pitts, B. J. *J. Phys. Chem. A* **2001**, *105*, 10339.
(5) Laskin, A.; Iedema, M. J.; Cowin, J. P. *Environ. Sci. Technol.* **2002**, *36*, 4948.
(6) Rivera-Figueroa, A. M.; Sumner, A. L.; Finlayson-Pitts, B. J. *Environ. Sci. Technol.* **2003**, *37*, 548.
(7) Ramazan, K. A.; Wingen, L. M.; Miller, Y.; Chaban, G. M.; Gerber, R. B.; Xantheas, S. S.; Finlayson-Pitts, B. J. *J. Phys. Chem. A* **2006**, *110*, 6886.
(8) Soule, M. C. K.; Blower, P. G.; Richmond, G. L. *J. Phys. Chem. A* **2007**, *111*, 3349.
(9) Shamay, E. S.; Buch, V.; Parrinello, M.; Richmond, G. L. *J. Am. Chem. Soc.* **2007**, *129*, 12910.
(10) Wang, S. Z.; Bianco, R.; Hynes, J. T. *J. Phys. Chem. A* **2009**, *113*, 1295.
(11) Bianco, R.; Wang, S. Z.; Hynes, J. T. *J. Phys. Chem. A* **2007**, *111*, 11033.
(12) Hüfner, S. *Photoelectron Spectroscopy: Principles and Applications*; Springer-Verlag: New York, 1995.
(13) Ottosson, N.; Faubel, M.; Bradforth, S. E.; Jungwirth, P.; Winter, B. *J. Electron Spectrosc. Relat. Phenom.* **2010**, *177*, 60.
(14) Winter, B. *Nucl. Instrum. Methods Phys. Res., Sect. A* **2009**, *601*, 139.
(15) Lewis, T.; Winter, B.; Stern, A. C.; Baer, M. D.; Mundy, C. J.; Tobias, D. J.; Hemminger, J. C. *J Phys. Chem. B* **2011**, *115*, 9445–9451.
(16) VandeVondele, J.; Krack, M.; Mohamed, F.; Parrinello, M.; Chassaing, T.; Hutter, J. *Comput. Phys. Commun.* **2005**, *167*, 103.
(17) Goedecker, S.; Teter, M.; Hutter, J. *Phys. Rev. B* **1996**, *54*, 1703.
(18) Grimme, S. *J. Comput. Chem.* **2006**, *27*, 1787.
(19) Becke, A. D. *Phys. Rev. A* **1988**, *38*, 3098.
(20) Lee, C. T.; Yang, W. T.; Parr, R. G. *Phys. Rev. B* **1988**, *37*, 785.
(21) Mundy, C. J.; Kuo, I. F. W.; Tuckerman, M. E.; Lee, H. S.; Tobias, D. J. *Chem. Phys. Lett.* **2009**, *481*, 2.
(22) Schmidt, J.; VandeVondele, J.; Kuo, I. F. W.; Sebastiani, D.; Siepmann, J. I.; Hutter, J.; Mundy, C. J. *J. Phys. Chem. B* **2009**, *113*, 11959.
(23) Yoo, S; Xantheas, S. S. *J. Chem. Phys.* **2011**, *134*, 121105.
(24) Kuehne, T. D.; Pascal, T. A.; Kaxiras, E; Jung, Y. *J. Phys. Chem. Lett.* **2011**, *2*, 105.
(25) Baer, M. D.; Mundy, C. J. *J. Phys. Chem. Lett.* **2011**, *2*, 1088.

(26) Kuo, I.-F. W.; Mundy, C. J. *Science* **2004**, *303*, 658.
(27) Mundy, C. J.; Kuo, I. F. W. *Chem. Rev.* **2006**, *106*, 1282.
(28) Martyna, G. J.; Klein, M. L.; Tuckerman, M. *J. Chem. Phys.* **1992**, *97*, 2635.
(29) Winter, B.; Aziz, E. F.; Hergenhahn, U.; Faubel, M.; Hertel, I. V. *J. Chem. Phys.* **2007**, *126*, 124504.